Optimal Configuration of Shared Energy Storage in Multi-Microgrids

Yining Zhang [1], Guanzhen Wang [2,*], Shucan Zhou [1], Xianfu Gong [1], Yong Lin [1], Weijie Wu [1], and Suhua Lou [2]

[1] Grid Planning and Research Center, Guangdong Grid Co., Ltd., Guangzhou, 510000, China;

[2] State Key Laboratory of Advanced Electromagnetic Engineering and Technology (Huazhong University of Science and Technology), Wuhan, 430074, China.

Abstract. An optimization model is proposed in this paper to allocate shared energy storage within multi-microgrids (MMGs). The model comprehensively considers system operation costs, energy storage allocation costs, and incorporates tiered carbon trading costs into the optimization objective, aiming to minimize overall system costs while maximizing carbon reduction benefits. Additionally, the Big-M method is employed to transform nonlinear constraints into a linear form, and case studies of specific MMGs systems are analyzed to validate the significant economic and environmental advantages of shared energy storage stations compared to individually allocated storage for each microgrid. Furthermore, the paper provides an in-depth discussion on the optimal configuration schemes, economic costs, and the impacts on carbon trading under varying scales of renewable energy integration. These findings offer theoretical insights for the optimal deployment of shared energy storage in the future development of power systems.

Keywords: Multi-microgrids; Shared Energy Storage; Energy Storage Optimal Allocation; Big-M method; Tiered Carbon Trading.

1. Introduction

With the continuous development of the global economy, the depletion of traditional fossil fuels and the intensifying environmental pollution have emerged as increasingly critical concerns. These issues not only pose a significant threat to the global ecosystem but also hinder sustainable economic growth. Consequently, clean and renewable energy sources, including wind and solar power, have emerged as crucial forces driving the shift toward more sustainable energy systems, owing to their environmentally friendly properties and limitless availability. However, the inherent variability and unpredictability of these renewable resources add substantial complexity to the operation of microgrid (MG) [1-2]. MG, which is a self-sufficient energy system integrating distributed generation, energy storage, and load, offers notable flexibility and adaptability. This system improves energy efficiency by utilizing locally generated renewable energy. Despite this, a single MG faces limitations in fully integrating renewable energy and achieving a balanced energy supply and demand, making the task of optimizing power distribution challenging. To overcome this, the multi-microgrids (MMGs) concept has been proposed. By enabling the collaborative operation of several microgrids, MMGs enhance the overall reliability of power supply and optimize energy utilization across the system [3-4].

Furthermore, energy storage technology plays a vital role in mitigating renewable energy generation fluctuations and improving system flexibility, thereby supporting the integration of renewables into the grid. However, the substantial costs involved in establishing standalone energy storage systems pose a major barrier to their widespread adoption in grids with significant renewable energy penetration [5]. Recently, the concept of the sharing economy has been introduced and rapidly developed. Relying on internet and information communication technologies, the sharing economy innovatively separates the ownership and usage rights of resources. Through models such as leasing and borrowing, the usage rights of resources can flow flexibly between different participants, thereby maximizing resource utilization efficiency [6-7]. This sharing model helps reduce resource idle time, effectively control usage costs, and, in turn, drives the diversified

development and innovation of the social economy. This concept has been successfully integrated into the energy storage sector, leading to the emergence of shared energy storage systems. It not only lower the capital costs of energy storage installation but also improve the operational efficiency of the system. Hence, both theoretically and practically, exploring the energy storage needs of multi-microgrid systems and optimizing the allocation of shared energy storage resources is crucial. Such research holds the potential to significantly boost renewable energy utilization while lowering the overall operational costs of the system [8].

In recent years, the optimization and economic aspects of shared energy storag systems have been explored by many researchers. Reference [9] tackles the uncertainties associated with renewable energy generation and load demand, determines the optimal storage capacity configuration by employing multi-stage stochastic programming (MSP). Reference [10] uses genetic algorithms to optimize energy storage capacity while enabling the sharing of surplus electricity and storage resources among community users. Reference [11] considers both storage capacity and power, proposing a non-cooperative game approach for optimal storage allocation. Reference [12] presents the concept of "cloud energy storage" and provides a comprehensive analysis of its key business models, investment strategies, and operational methods. Additionally, Reference [13] examines the control methods, communication technologies, and operational principles of cloud energy storage, validating its economic and technical viability through an analysis of Ireland's power system. Reference [14] presents a novel energy-sharing cloud mechanism for smart microgrids, which combines energy storage and renewable energy features to support energy-sharing services between multiple parties using virtual producer-consumer relationships. Reference [15] investigates battery lifespan and demand response in microgrids and proposes a hybrid energy storage optimization method that significantly lowers power supply costs in remote areas. Reference [16] develops a distributed robust game-based optimization method for scheduling microgrid clusters with shared energy storage, enhancing system economics while ensuring privacy and security. Reference [17] introduces a framework for coordinating different energy storage systems, utilizing shared energy storage stations to alleviate transmission network congestion and improve distribution grid economics. Reference [18] focuses on energy storage allocation and operation in electricity-hydrogen hybrid energy storage multi-microgrid systems, using the grey wolf-sine cosine optimization algorithm to validate the model. Finally, Reference [19] constructs an energy trading system for a neighborhood network comprising shared energy storage providers, non-dispatchable generation users, and electricity retailers, aiming to maximize shared energy storage providers' profits and minimize social costs at the user level through demand-side management.

In summary, research on SES is still in its infancy. Current research primarily concentrate on the configuration strategies and business models of SES systems, there is a lack of comprehensive analysis regarding the charging and discharging behaviors, as well as the role of SES in carbon reduction and carbon trading within multi-microgrids (MMGs). To address this gap, this paper introduces an optimization model for the allocation of shared energy storage in MMGs. The model considers system operation costs, energy storage allocation costs, and integrates tiered carbon trading costs into the optimization objective, with the goal of minimizing costs and maximizing carbon reduction benefits. In addition, the Big-M method is employed to transform nonlinear constraints into a linear form, and studies of specific MMGs are also provided to highlight the distinct economic and environmental advantages of shared energy storage stations over individual storage systems for each MG. Additionally, the paper discusses the optimal SES configuration, economic costs, and the effects on carbon trading for varying levels of renewable energy integration. These findings offer theoretical insights for the optimal deployment of shared energy storage in the future development of power systems.

2. Multi-Microgrids with Shared Energy Storage Stations

The energy storage services are offered by the SES station to MMGs within the same distribution grid. Each MG can leverage this shared resource to fulfill its charging and discharging requirements, effectively overcoming the time and capacity limitations of standalone storage systems. The structure of a multi-microgrids (MMGs) system with SES comprises the distribution network, the MGs, and the shared storage facility, as depicted in Figure 1.

In this system, the primary units connected to both the distribution grid and the shared energy storage (SES) station are the MMGs. Each MG consists of wind turbines (WT), photovoltaic panels (PV), and micro gas turbines (MT), with all MGs relying on a single SES unit. When renewable energy production within the MMGs is insufficient to meet demand, can restore balance by either discharging the SES, purchasing power from the distribution network, or utilizing MT. Conversely, when individual MGs generate excess renewable energy, it can be used to charge the shared storage, thus improving the overall utilization of renewable energy.

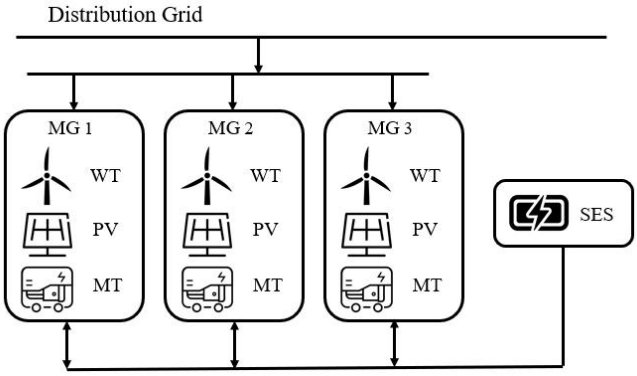

Fig. 1 System architecture of MMGs with SES

The SES station captures excess electricity generated by the MG and provides discharge services as needed. It makes use of any residual energy within the station to support discharging for microgrids and can transfer surplus electricity from microgrids with charging needs to others requiring discharge. Evaluating the load demand of each MG during the operational cycle, the station determines the required storage capacity and the maximum charge/discharge power. Once a cycle is completed, the storage level resets to its initial state, ensuring readiness for the next cycle. This flexible scheduling of the SES enhances energy utilization efficiency within the MMGs while ensuring that each microgrid's load requirements are met.

3. Model Construction

3.1 Objective Function

(1) Total cost of the MMGs

The objective function of the model is to minimize the total cost of the MMGs. The operating costs of the MMGs include the operating cost of the MT, the purchase cost of electricity, the operating cost of the SES, the investment costs of the SES, and the carbon trading costs.

$$\min F = F_{MT} + F_{Buy} + F_{SES} + F_I + F_C \tag{1}$$

Where F represents the total cost of the MMGs; F_{MT} denotes the operating cost of the MT; F_{Buy} represents the cost of electricity purchased by the system; F_{SES} is the operating cost of the SES station; F_I denotes the investmen cost of the SES station; and F_C represents the carbon trading cost of the MMGs.

(2) Operating cost of the MT

$$F_{MT} = \sum_{t=1}^{T}\sum_{i=1}^{N}\frac{P_{MT,i,t}}{\eta_{MT,i}H}\gamma_t \tag{2}$$

Where T represents the scheduling time; N denotes the number of MT; $P_{MT,i,t}$ is the output of MT i in time period t; $\eta_{MT,i}$ represents the efficiency of the MT; H is the higher heating value of natural gas; and γ_t is the unit price of natural gas in time period t.

(3) Purchase cost of electricity

$$F_{Buy} = \sum_{t=1}^{T}\sum_{i=1}^{N}P_{Buy,i,t}\gamma_t \tag{3}$$

Where $P_{Buy,i,t}$ represents the purchased power of MG i in time period t; γ_t denotes the electricity price in time period t.

(4) Operating cost of the shared energy storage station

$$F_{SES} = \sum_{t=1}^{T}\sum_{i=1}^{N}(P_{b,i,t} + P_{s,i,t})\delta_{SES} \tag{4}$$

Where $P_{b,i,t}$ represents the discharging power of the SES used by MG i in time period t; $P_{s,i,t}$ represents the charging power of the SES used by MG i in time period t; δ_{SES} denotes the unit operating cost of the SES station.

(5) Investmen cost of the shared energy storage station

$$F_I = c_e E_{SES} + c_p P_{SES} \tag{5}$$

Where E_{SES} represents the rated capacity of the SES; P_{SES} denotes the rated power of the SES; c_e is the unit capacity cost of the SES; c_p is the unit power cost of the SES.

(6) Carbon trading cost of the MMGs

$$F_C = \begin{cases} -c(2+\beta)d - c(1+2\beta)\left(-2d - E_t\right), & E_t \le -2d \\ -cd - c\left(1+\beta\right)\left(-d - E_t\right), & -2d < E_t \le -d \\ cE_t, & -d < E_t \le 0 \\ cE_t, & 0 < E_t \le d \\ cd + c(1+\beta)\left(E_t - d\right), & d < E_t \le 2d \\ c(2+\beta)d + c(1+2\beta)\left(E_t - 2d\right), & E_t > 2d \end{cases} \tag{6}$$

$$E_t = E_p - E_q \tag{7}$$

$$E_p = \sum_{t=1}^{T}\sum_{i=1}^{N}(\chi_{g,i}P_{g,i,t} + \chi_{B,i}P_{B,i,t}) \tag{8}$$

$$E_q = \sum_{t=1}^{T}\sum_{i=1}^{N}(\theta_{g,i}P_{g,i,t} + \theta_{B,i}P_{B,i,t}) \tag{9}$$

Where d is the interval length of carbon emissions; β denotes the growth rate of carbon trading prices; c is the baseline price for the system's carbon emission trading; E_t represents the system's carbon trading volume; E_p is the system's carbon emissions; E_q denotes the system's carbon allowance; $\chi_{g,i}$ and $\chi_{B,i}$ are the carbon emission coefficients for MT *i* and grid power purchases in MG *i,* respectively; $\theta_{g,i}$ and $\theta_{B,i}$ are the carbon allowance coefficients for MT *i* and grid power purchases in MG *i*, respectively.

3.2 Constraints

(1) Power balance constraint

$$P_{PV,i,t} + P_{WT,i,t} + P_{MT,i,t} + P_{Buy,i,t} + P_{b,i,t} - P_{s,i,t} = P_{L,i,t} \tag{10}$$

Where $P_{PV,i,t}$ represents the photovoltaic power of MG *i* in time period *t*; $P_{WT,i,t}$ denotes the wind power of MG *i* in time period *t*; $P_{L,i,t}$ is the load power of MG *i* in time period *t*.

(2) MT output upper and lower bound constraint

$$0 \le P_{MT,i,t} \le P_{MT,i,\max} \tag{11}$$

Where $P_{MT,i,\max}$ represents the rated power of MT *i*.

(3) MT output ramp-up constraint

$$-r_{MT,i,down} \le P_{MT,i,t} - P_{MT,i,t-1} \le r_{MT,i,up} \tag{12}$$

Where $r_{MT,i,up}$ and $r_{MT,i,down}$ represent the maximum ramp-up rate and ramp-down rate of output of MT *i*, respectively.

(4) Charging and discharging power constraints for MG using SES stations

$$\begin{cases} 0 \le P_{b,i,t} \le P_{b,i,\max}U_{b,i,t} \\ 0 \le P_{s,i,t} \le P_{s,i,\max}U_{s,i,t} \\ U_{b,i,t} + U_{s,i,t} \le 1 \end{cases} \tag{13}$$

Where $P_{b,i,\max}$ and $P_{s,i,\max}$ represent the maximum discharging and charging power values, respectively, that MG *i* can use from the SES station; $U_{b,i,t}$ is the discharging status of MG *i* in time period *t*, where 0 indicates no discharging and 1 indicates discharging; $U_{s,i,t}$ is the charging status of MG *i* in time period *t*, where 0 indicates no charging and 1 indicates charging.

(5) State of charge (SOC) constraints for shared energy storage stations

$$\begin{cases} E_{SES,t} = E_{SES,t-1} + (\eta_{SES,s} P_{SES,s,t} - \dfrac{P_{SES,b,t}}{\eta_{SES,b}}) \\ \omega_1 E_{SES} \leq E_{SES,t} \leq \omega_2 E_{SES} \end{cases} \tag{14}$$

Where $E_{SES,t}$ represents the energy of the SES in time period *t*, $\eta_{SES,s}$ and $\eta_{SES,b}$ denote the charging efficiency and discharging efficiency of the SES, respectively; $P_{SES,s,t}$ and $P_{SES,b,t}$ represent the charging and discharging power of the SES, respectively; ω_1 and ω_2 are the minimum and maximum SOC of the SES, respectively.

(6) Charging and discharging power constraints for shared energy storage stations

$$\begin{cases} 0 \leq P_{SES,b,t} \leq P_{SES} U_{SES,b,t} \\ 0 \leq P_{SES,s,t} \leq P_{SES} U_{SES,s,t} \\ U_{SES,b,t} + U_{SES,s,t} \leq 1 \end{cases} \tag{15}$$

Where $U_{SES,b,t}$ represents the discharging status of the SES at time *t*, where 0 indicates no discharging and 1 indicates discharging; $U_{SES,s,t}$ represents the charging status of the SES at time *t*, where 0 indicates no charging and 1 indicates charging..

(7) Charging and discharging power balance constraints for shared energy storage stations

$$\sum_{i=1}^{N} (P_{b,i,t} - P_{s,i,t}) = P_{SES,b,t} - P_{SES,s,t} \tag{16}$$

(8) Purchased power constraint for MG

$$0 \leq P_{Buy,i,t} \leq P_{Buy,i,\max} \tag{17}$$

Where $P_{Buy,i,\max}$ represents the maximum purchased power of MG *i*.

3.3 Solution Method

By examining all the constraints, it can be observed that constraint (15) is nonlinear. In order to linearize it, applying the Big-M method is feasible, which can transform it into constraint (18).

$$\begin{cases} 0 \leq P_{SES,b,t} \leq P_{SES} \\ 0 \leq P_{SES,b,t} \leq U_{SES,b,t} M \\ 0 \leq P_{SES,s,t} \leq P_{SES} \\ 0 \leq P_{SES,s,t} \leq P_{SES} M \\ U_{SES,b,t} + U_{SES,s,t} \leq 1 \end{cases} \tag{16}$$

Where *M* is a sufficiently large constant.

After linearizing the nonlinear constraints, the SES optimization model of the MMGs is transformed into a mixed-integer linear programming problem. This problem can be solved by using the commercial solver Gurobi and the Yalmip toolbox in Matlab 2021.

4. Case Study Analysis

4.1 Introduction to the Case Study System

A case study is conducted using a MMGs system as an example. The MMGs system consists of three MG (MG1, MG2, and MG3), with the renewable energy output and load curves for each MG on a typical day shown in Fig. 2-4. The electricity purchase prices and natural gas prices for each MG are illustrated in Fig. 5. Each MG is equipped with a 50 kW MT, with a ramp-up/down rate of 50 kW/h, an efficiency of 40%, and a calorific value of 9.7 kW·h/m³. The minimum and maximum SOC for the SES are 0.1 and 0.9, respectively, with an initial SOC of 0.2. The operational cost is ￥0.30/(kW·h). The maximum discharging and charging power for the SES station used by each MG is 1000 kW, with a capacity cost of ￥1200/(kW·h) and a power cost of ￥1000/(kW). The maximum electricity purchasing power for each MT is limited to 100 kW. The carbon emission coefficients for the MT and electricity purchasing are 0.7246 kg/(kW·h) and 1.08 kg/(kW·h), respectively. The carbon allocation coefficients are 0.424 kg/(kW·h) and 0.728 kg/(kW·h), respectively. The carbon emission value range length is 360 kg. The carbon trading price growth rate is 0.5, and the baseline carbon emission rights trading price for the system is ￥0.12/kg.

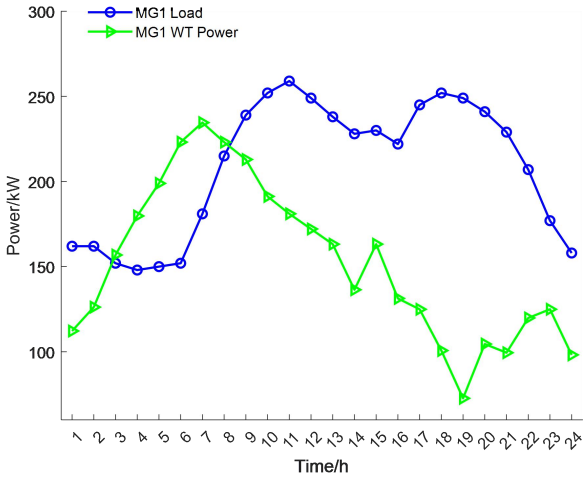

Fig. 2 Renewable energy output and load curve of MG1

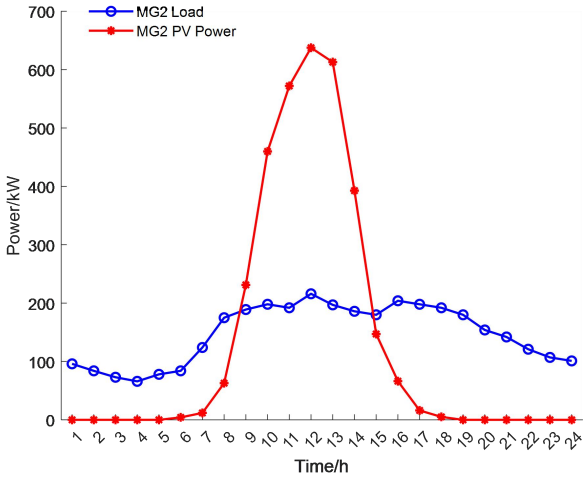

Fig. 3 Renewable energy output and load curve of MG2

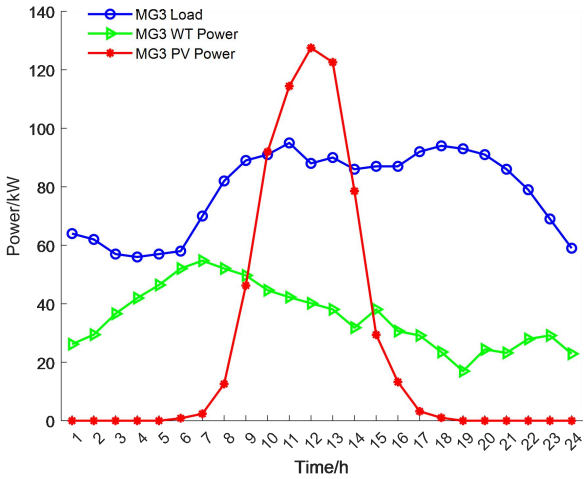

Fig. 4 Renewable energy output and load curve of MG3

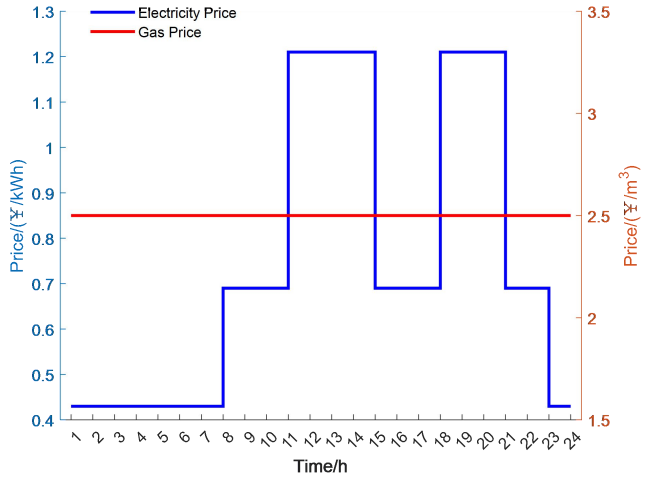

Fig. 5 Electricity price and gas price curves

4.2 Optimization Results of Shared Energy Storage Station Configuration

Fig 6-8 present the power balance and carbon trading curves for each MG..

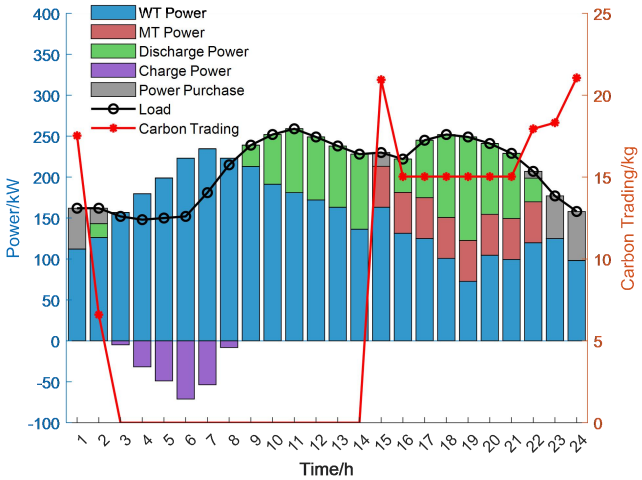

Fig. 6 Power balance and carbon trading curves of MG1

As shown in Fig 6, during the 3-8h period, MG1's wind power output exceeds the load, with the surplus wind energy being stored in the SES. In other periods, the wind power output falls short of meeting the load. From 2h, 9-14h, and 16-22h, the SES station discharged a significant amount of power to MG1. The discharge power reached its maximum of 126.325 kW at 19h, when the wind power output was at its lowest. From 15-22h, the MT generated power, and during 1-2h, 15h, and 22-24h, electricity was purchased from the distribution grid. Additionally, the carbon trading curve indicates that MG1 purchased carbon allowances during 1-2h and 15-24h. At 24h, the system's electricity purchasing power peaked at 59.825 kW, and at this time, the highest carbon allowance purchase amount of 21.0584 kg was also made.

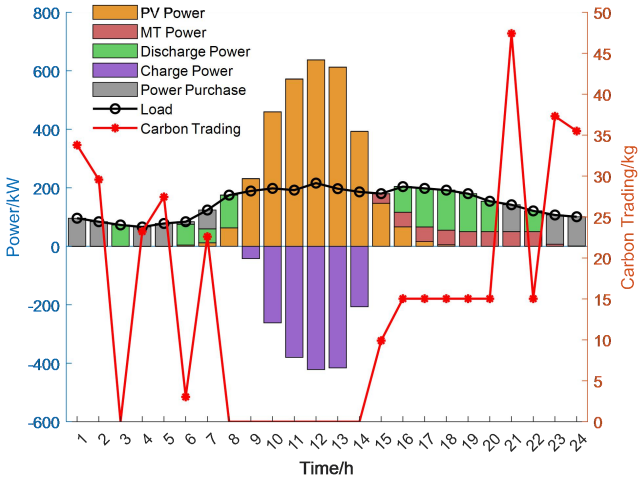

Fig. 7 Power balance and carbon trading curves of MG2

As shown in Fig 7, during the 9-14h period, the photovoltaic output of MG2 exceeds the load demand, and the SES station stores a large amount of surplus photovoltaic energy. The SES station discharged to MG2 during 3h, 6-8h, 16-20h, and 22h. From 15-23h, the MT generated power, and during 1-2h, 4-7h, 21h, and 23-24h, electricity was purchased from the distribution grid. MG2 purchased carbon allowances during 1-2h, 4-7h, and 15-24h. At 21h, the system's power supply was entirely met by the MT and electricity purchased from the grid, with the carbon allowance purchase reaching the maximum value of 47.414 kg for the day.

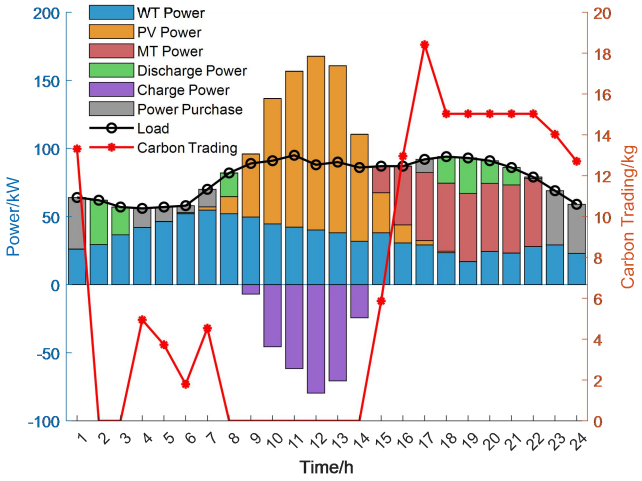

Fig. 8 Power balance and carbon trading curves of MG3

As depicted in Fig 8, during 9-14h period, the renewable energy output of MG3 exceeds the load demand, and the SES station stores a substantial amount of it. During 2-3h, 8h, and 18-21h periods, the SES station released a small quantity of energy to MG3. During 15-22h, the MT generated power, and during 1h, 4-7h, 17h, and 23-24h, electricity was purchased from the distribution grid.

Additionally, MG3 purchased carbon allowances during 1h, 4-7h, and 15-24h. At 17h, when the load was high and the clean power supply was low, the MT output was kept at its maximum, and the system purchased electricity, which caused the carbon allowance purchase to reach its maximum value of 18.4145 kg.

Fig 9 illustrates the charge/discharge power and SOC curves of the SES.

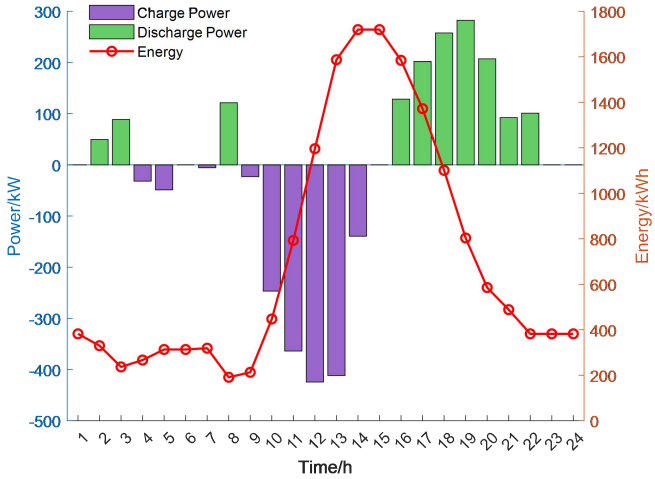

Fig. 9 The charge / discharge power and SOC curves of the SES

As shown in Fig 9, the SES station discharges during 2-3h, with the energy level dropping to 236.702 kW·h. It charges from 4-5 hours and 7 hours, with the energy level rising to 318.785 kW·h. Later, during the 8th hour, it discharges again, and the energy level drops to the lowest point of the day, 191.067 kW·h. During 9-14 hours, the SES remains in a continuous charging state, storing the excess renewable energy from the MMGs. The maximum charging power occurs at 12 hours, reaching 424.287 kW, and the energy level rises to its maximum of 1719.6 kW·h by 14 hours. From 16-22 hours, the station is in a continuous discharging state. The maximum discharging power occurs at 19 hours, reaching 282.368 kW, and the energy level decreases to the minimum value of 382.133 kW·h by 22 hours. The SOC keeps the initial value of 0.2 during 22-24h, allowing the SES system to enter the next operating cycle.

By treating MG1、MG2 and MG3 as a whole, the power balance and carbon trading curves of MMGs can be obtained, as shown in Fig 10.

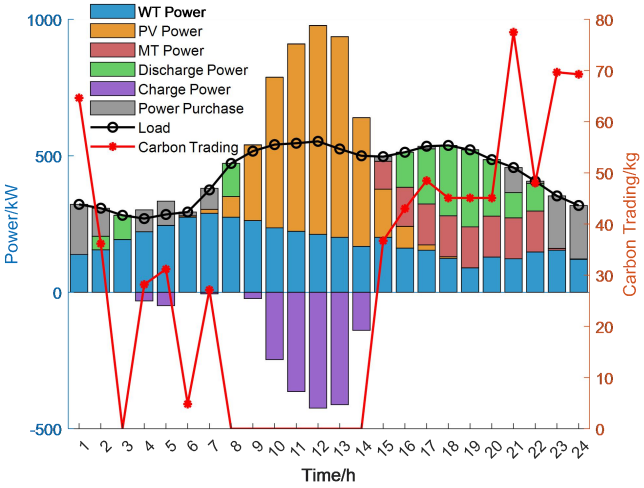

Fig. 10 Power balance and carbon trading curves of MMGs

As shown in Fig 6 to 10, the power distribution of SES in the MMGs system is balanced throughout the day. By flexibly adjusting the charging and discharging power according to the

renewable energy output and load characteristics of each MG, SES promotes renewable energy consumption while maintaining the power balance of each MG.

4.3 Analysis of Different Energy Storage Station Configuration Schemes

Two scenarios are considered for comparative analysis in order to evaluate the economic and environmental benefits of SES stations:

Scenario 1: Each MG configures its own energy storage system independently;

Scenario 2: The MMGs share a common energy storage system.

In Scenario 1, each MG prioritizes the utilization of its renewable energy generation based on its internal load demand characteristics, while also factoring in micro gas turbine generation and electricity purchases from the distribution network. They independently configure their own energy storage capacity and rated power. Presented in Table 1 are the results of the independent energy storage configuration for each MG, with the associated configuration costs detailed in Table 2.

Table 1. The independent energy storage planning results for each MG

Category	Energy Storage Capacity (kW·h)	Rated Power (kW)
MG1	259.2906	71.125
MG2	2052.1781	421.5
MG3	343.0183	79.6625
MMGs	2654.487	572.2875

Table 2. Independent Energy Storage Planning Cost for MMGs Unit: ¥

Total Cost	MT Operating Cost	Electricity Purchase Cost	Carbon Trading Cost	Energy Storage Operating Cost	Energy Storage Investment Cost
3760455.0159	551.4535	832.0265	112.6919	1286.9066	3757671.9375

In Scenario 2, shown in Table 3 are the SES configuration results in Scenario 2, with the configuration costs presented in Table 4..

Table 3. SES configuration results for MMGs

Category	Energy Storage Capacity (kW·h)	Rated Power (kW)
MMGs	1910.6667	424.2875

Table 4. SES planning cost for MMGs Unit: ¥

Total Cost	MT Operating Cost	Electricity Purchase Cost	Carbon Trading Cost	Energy Storage Operating Cost	Energy Storage Investment Cost
2719052.3915	722.127	488.8898	108	645.8122	2717087.5625

A comparison between Table 3 and Table 1, as well as Table 4 and Table 2, reveals that after integrating the SES station, the MMGs total installed storage capacity decreased by 28.02%, and the configured power dropped by 25.86%. Moreover, the total investment cost for energy storage was reduced by 27.69%, resulting in an overall system cost reduction of 27.69%. This demonstrates the considerable economic benefits of adopting SES..

In terms of system energy cleanliness, although the integration of the SES led to a 30.95% increase in the operating cost of MT, while the cost of purchasing electricity decreased by 41.24%, easing the load on the main grid. This also resulted in a 12.47% reduction in the cost of using non-clean energy. Additionally, considering tiered carbon trading, the carbon trading cost decreased

by 4.16%. This demonstrates that SES can lower the overall carbon quota required by the system, supporting energy conservation, emissions reduction, and improving system cleanliness.

4.4 Analysis of Shared Energy Storage Configuration Costs under Different Renewable Energy Penetration Scenarios

As the economy and society progress, the share of renewable energy installations continues to grow, making the shift toward cleaner power generation structures in the electricity system more apparent. To assess the configuration costs of SES stations at varying levels of renewable energy integration, the renewable energy installed capacity for each grid is increased by 5%, 10%, 15%, 20%, and 25%, creating five distinct scenarios for analysis. Figures 11 and 12 illustrate the SES configuration and operational costs for the MMGs across these scenarios.

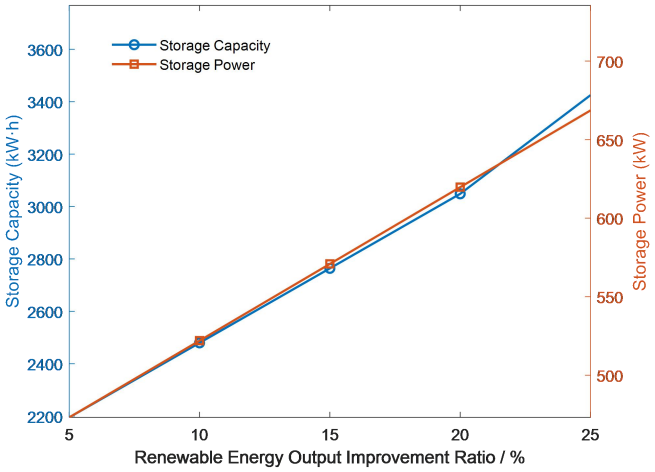

Fig. 11 The configuration of SES station capacity and rated power under different renewable energy penetration improvement ratio

As shown in Fig. 11, as the proportion of renewable energy installations rises, both the configured capacity and power of SES increase, indicating a positive correlation. This is due to the greater fluctuations in renewable energy output, which lead to a larger peak-to-valley difference in the system's net load. Consequently, more energy storage is required. The power distribution between microgrids must be coordinated according to each microgrid's source-load characteristics to ensure system-wide power balance.

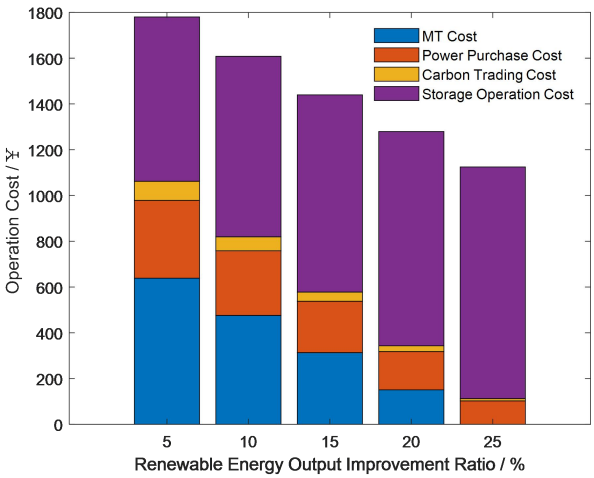

Fig. 12 Operation costs of MMGs under different renewable energy penetration improvement ratio

As shown in Fig. 12, with the increase in renewable energy installations, the operational costs of MMGs decrease significantly. Specifically, costs related to micro gas turbines, electricity purchases,

and carbon trading all decline, with the micro gas turbine operating cost reaching zero when renewable energy penetration increases by 25%. This is due to the high costs and carbon emissions associated with micro gas turbine generation and electricity purchases, which negatively affect the system's economic and environmental performance. In contrast, renewable energy, being low-cost and clean, can effectively replace these sources.

At the same time, the operational cost of the SES station rises. This is because while the operating cost of energy storage is lower than that of MT and electricity purchases, and it does not generate carbon emissions, its usage increases. To maintain power balance across the MMGs, the SES's charging and discharging power is utilized more intensively, resulting in a rise in its operational cost.

5. Summary

This paper develops an optimized configuration model for SES in MMGs. Using a MMGs composed of three MG as a case study, a detailed analysis is conducted. The research findings are as follows:

(1) The proposed model can determine the optimal configuration and charge/discharge strategy for SES in MMGs, as well as the charge/discharge strategies for each MG, micro-turbine operation schemes, electricity purchase plans from the distribution grid, and carbon trading strategies. By considering the source-load characteristics of each MG, the model ensures the economically efficient operation of the MMGs.

(2) When compared to configuring independent energy storage for each MG, implementing SES stations in MMGs reduces the capacity and rated power requirements for energy storage. This not only enhances the system's economic performance but also reduces reliance on non-clean energy, thereby contributing to enhance the system cleanliness.

(3) With an increase in renewable energy integration within MMGs, the required capacity and power of SES also grow, enhancing the efficient utilization of renewable energy and allows for more effective power distribution through optimized charging and discharging.

References

[1] LI Shuang, SHI Yixiang, CAI Ningsheng. Advances in hydrogen production from fossil and renewable energy sources for energy transition[J]. Journal of Tsinghua University (Natural Science Edition), 2022, 62(4): 655-662.

[2] LIU Yongqi, CHEN Longxiang, HAN Xiaoqi. Analysis of key issues of new energy substitution in China under energy transition[J]. Chinese Journal of Electrical Engineering, 2022, 42(2): 515-524.

[3] SAN Bo, ZHANG Tao, LIU Yajie, et al. A review of energy management systems for multi-microgrids[J]. Chinese Journal of Electrical Engineering, 2020, 40(10): 3077-3093.

[4] WU Xiong, WANG Xiuli, LIU Shimin, et al. Research review on energy management system for microgrid[J]. Power Automation Equipment, 2014, 34(10): 7-14.

[5] MA Li, Li Wei, Pei Wei, et al. Optimization of hybrid energy storage allocation with high percentage of photovoltaic distribution network metering and demand side response[J/OL]. High Voltage Technology: 1-9.

[6] 10 CAI S J，LONG X L，LI L，et al． Determinants of intention and behavior of low carbon commuting through bicycle-sharing in China ［J］． Journal of Cleaner Production，2019，212: 602-609．.

[7] YANG Xuecheng， TU Ke． Research on the dynamic value cocreation in the sharing economic background: A case study of the travel platform［J］． Management Review，2016，28(12) : 258-268．

[8] LI Xianshan, XIE Shijie, FANG Zijian, et al. Optimal allocation of shared energy storage in multiple microgrids and its cost sharing[J]. Power Automation Equipment, 2021, 41(10): 44-51

[9] Hafiz F, Rodrigo De Queiroz A, Fajri P, Husain I. Energy Management and Optimal Storage Sizing for a Shared Community: A Multi-Stage Stochastic Programming Approach [J]. Applied Energy, 2019, 236: 42-54.

[10] Huang P, Sun Y, Lovati M, Zhang X. Solar-Photovoltaic-Power-Sharing-Based Design Optimization of Distributed Energy Storage Systems for Performance Improvements [J]. Energy, 2021, 222.

[11] Xiao J-W, Yang Y-B, Cui S, Liu X-K. A New Energy Storage Sharing Framework with Regard to Both Storage Capacity and Power Capacity [J]. Applied Energy, 2022, 307.

[12] KANG Chongqing，LIU Jingkun，ZHANG Ning．A new form of energy storage in future power system: Cloud energy storage［J］．Automation of Electric Power Systems，2017，41(21) : 2-8，16．

[13] LIU J K，ZHANG N，KANG C Q，et al．Cloud energy storage for residential and small commercial consumers: A business case study ［J］．Applied Energy，2017，188: 226-236．

[14] Li S, Zhu J, Dong H. A novel energy sharing mechanism for smart microgrid[J]. IEEE Transactions on Smart Grid, 2021, 12(06): 5475-5478.

[15] YANG Xiaohui,YUAN Zhixin,XIAO Jinyang,et al. Optimal configuration of hybrid energy storage microgrid considering battery life[J]. Power System Protection and Control,2023,51(04):22-31.

[16] ZANG Yunfan, Xia Sheng, Li Jiawen, et al. Optimal scheduling method of microgrid cluster distribution robust game with shared energy storage[J]. Power System Protection and Control,2023,51(24):90-101.

[17] Elliott R T, Fernandez-Blanco R, Kozdras K, et al. Sharing energy storage between transmission and distribution[J]. IEEE Transactions on Power Systems, 2018, 34(01): 152-162.

[18] LI Ruirui,LI Qi,PU Yuchen,et al. Optimal capacity allocation of multiple microgrid systems with hybrid electric-hydrogen energy storage taking into account power interaction constraints[J]. Power System Protection and Control,2022,50(14):53-64.

[19] Mediwaththe C P, Shaw M, Halgamuge S, et al. An incentive-compatible energy trading framework for neighborhood area networks with shared energy storage[J]. IEEE Transactions on Sustainable Energy, 2019, 11(01): 467-476.